

GUEST COMMENTARIES

Diffusion in Biofilms

Philip S. Stewart*

Center for Biofilm Engineering and Department of Chemical Engineering, Montana State University–Bozeman, Bozeman, Montana, 59717-3980

Much of what makes life in a microbial biofilm different from life in a free aqueous suspension can be explained by invoking the phenomenon of diffusion. This article discusses the profound influence of the physics of the diffusion process on the chemistry and biology of the biofilm mode of growth. I have framed the discussion in the form of answers to five important questions.

WHY IS DIFFUSION AN IMPORTANT PROCESS IN BIOFILMS?

When microorganisms are grown in planktonic culture, diffusion is usually of little consequence. There are two reasons for this. The first reason is that planktonic cultures are generally agitated, and the resulting fluid flow transports solutes rapidly, resulting in a well-mixed system. Transport that occurs as a solute is carried by the bulk flow of a fluid (convection) is generally much faster than the transport resulting from random molecular motion (diffusion). Of course, there is no net convective flow of fluid into or out of the microbial cell. At some point close to the cell, diffusion becomes critical for moving the solute toward or away from the cell surface. The reason that diffusion does not limit this step is that the diffusion distance is small and diffusion is rapid over such short distances.

Diffusion limitation arises readily in biofilm systems because fluid flow is reduced and the diffusion distance is increased in the biofilm mode of growth. The biofilm and the substratum to which it is anchored impede flow in the vicinity of the biofilm, throttling convective transport. Inside cell clusters, the locally high cell densities and the presence of extracellular polymeric substances arrest the flow of water. Diffusion is the predominant transport process within cell aggregates (7, 36). Whereas the diffusion distance for a freely suspended microorganism is of the order of magnitude of the dimension of an individual cell, the diffusion distance in a biofilm becomes the dimension of multicellular clusters. This can easily represent an increase in the diffusion distance, compared to a single cell, of 2 orders of magnitude. As is explained in the next section, diffusive equilibration time scales as the square of the diffusion distance. In other words, a biofilm that is 10 cells thick will exhibit a diffusion time 100 times longer than that of a lone cell.

HOW FAST DO SOLUTES DIFFUSE INTO OR OUT OF A BIOFILM?

Suppose a stain is added to the medium bathing a biofilm. How long will it take this dye to permeate, by diffusion, to the interior of a cell cluster or to the bottom of the biofilm? Because I aspire in this article to avoid overwhelming the reader with mathematics, I will define a single, simple measure of diffusive penetration time. There are two versions of this measure, depending on the geometry of the system. The time required for a solute added to the fluid bathing a biofilm to attain 90% of the bulk fluid concentration at the base of flat slab (uniformly thick) biofilm is given very simply by

$$t_{90} = 1.03 \frac{L^2}{D_e} \quad (1)$$

Here, L is the biofilm thickness, and D_e is the effective diffusion coefficient in the biofilm. The time required for a solute to attain 90% of the bulk fluid concentration at the center of a spherical biofilm cell cluster is given by

$$t_{90} = 0.37 \frac{R^2}{D_e} \quad (2)$$

where R is the cluster radius and D_e is the effective diffusion coefficient in the biofilm. The first step in performing these calculations is to estimate the effective diffusion coefficient in biofilm.

Biofilms are mostly water and the appropriate starting point for estimating a diffusion coefficient in a biofilm is to determine the value of the diffusion coefficient in pure water (D_{aq}). Some aqueous diffusion coefficients have been experimentally measured and can be found in the literature. Others can be estimated from a predictive correlation such as the Wilke-Chang correlation (22). Aqueous diffusion coefficients of selected solutes of interest in microbial systems are tabulated in Table 1. I have summarized elsewhere values of diffusion coefficients in water of various biocides and antibiotics (32, 34).

The diffusion coefficient in water depends on temperature, both directly and through the effect of temperature (T) on the solution viscosity (μ). This temperature dependence of aqueous diffusion coefficients can be calculated through the relationship $D_{aq}\mu/T = \text{constant}$.

The value of the effective diffusion coefficient in the biofilm will be reduced compared to the diffusion coefficient in water due to the presence of microbial cells, extracellular polymers, and abiotic particles or gas bubbles that are trapped in the biofilm. This reduction is described by the ratio D_e/D_{aq} . Ex-

* Mailing address: Center for Biofilm Engineering and Department of Chemical Engineering, Montana State University–Bozeman, Bozeman, Montana, 59717-3980. Phone: (406) 994-2890. Fax: (406) 994-6098. E-mail: phil_s@erc.montana.edu.

TABLE 1. Diffusion coefficients in water at 25°C

Solute	$10^{-6} D_{aq}$ in cm^2/s	Reference or source
Hydrogen	45.0	4
Nitrogen	18.8	4
Oxygen	20.0	10
Carbon dioxide	19.2	4
Methane	14.9	4
Ethane	12.0	4
Propane	9.7	4
Benzene	10.2	4
Hydrogen sulfide	16	22
Formic acid	14.1	4
Acetic acid	12.1	4
Propionic acid	10.6	4
Butyric acid	8.7	27
Benzoic acid	10.0	4
Succinic acid	9.4	4
<i>p</i> -Aminobenzoic acid	8.4	16
Fluorescein	5.4	— ^a
Methanol	15	16
Glycerol	9.4	22
Urea	13.8	4
Glucose	6.7	16
Sucrose	5.2	4
Lactose	4.9	22
Maltose	4.8	22
Raffinose	4.3	16
Glycine	11	16
Glutamine	7.6	16
Alanine	9.1	16
Leucine	7.3	16
Serine	8.8	16
Valine	8.3	4
Asparagine	8.3	16
Threonine	8.0	16
<i>N</i> -(3-Oxododecanoyl)-L-homoserine lactone	4.9	— ^a
<i>N</i> -Butyryl-L-homoserine lactone	7.2	— ^a
Li^+	10.3	16
NH_4^+	19.7	13
Cl^-	20.3	13
HCO_3^-	11.8	26
SO_4^{2-}	10.6	26
$\text{H}_2\text{PO}_4^{2-}$	8.8	18
HPO_4^-	7.6	18

^a —, estimated from the Wilke-Chang correlation as explained in reference 22.

perimental measurements of this ratio, termed the relative effective diffusivity, have been reviewed elsewhere (33) and that article presents guidelines and formulae for estimating D_e/D_{aq} in biofilms. There are also sophisticated approaches for calculating this ratio (40). The relative effective diffusivity depends on the biomass density in the biofilm and the physicochemical properties of the solute. D_e/D_{aq} in biofilm ranges from ca. 0.2 to 0.8 with a mean value of ca. 0.4. Figure 1 presents consensus values of D_e/D_{aq} for selected solutes. I suggest using a value of D_e/D_{aq} of 0.6 for light gases (e.g., oxygen, nitrous oxide, carbon dioxide, or methane) and a value of D_e/D_{aq} of 0.25 for most organic solutes.

Armed with an effective diffusion coefficient and an estimate of the biofilm thickness or cluster radius, the calculation of diffusive penetration times is straightforward. The best way to illustrate this is with some example calculations.

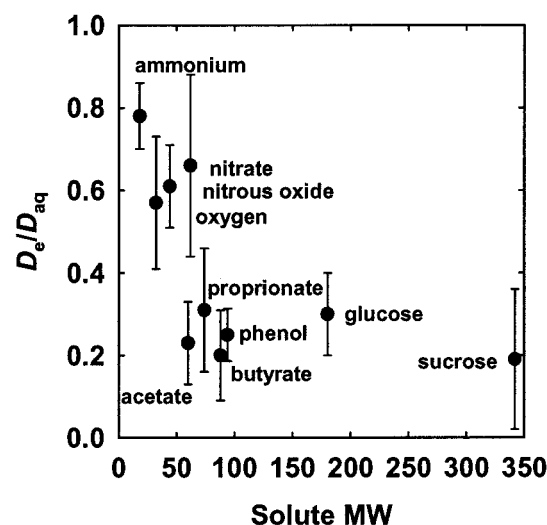


FIG. 1. Relative effective diffusion coefficients of selected solutes in biofilms. These values derive from a reanalysis of the data compiled by Stewart et al. (33). The error bars indicate the standard deviation.

Example calculation. A biofilm growing in a flow cell at room temperature (22°C) is to be stained with a fluorescein-tagged probe. The biofilm consists of tightly packed mushroom-shaped clusters that are 100 μm tall. How long must the sample be incubated with this reagent to ensure that the stain reaches to the full depth of the biofilm? Suppose that the diffusion coefficient of the fluorescent probe in water is half that of fluorescein, or $2.7 \times 10^{-6} \text{ cm}^2 \text{ s}^{-1}$ at 25°C. At 22°C this value becomes $2.5 \times 10^{-6} \text{ cm}^2 \text{ s}^{-1}$. Lacking specific information about the biofilm, we can take D_e/D_{aq} to be 0.25. This gives a value of D_e of $0.63 \times 10^{-6} \text{ cm}^2 \text{ s}^{-1}$. Though the biofilm is not uniformly thick, I will treat it as if it were. The result will be a conservative estimate of the required staining time. The diffusion time is $1.03L^2/D_e$, which equals 165 s. Staining for a few minutes should suffice.

Example calculation. Consider the penetration of a mouthwash into a roughly hemispherical patch of dental plaque with a radius of 260 μm . How long must one rinse with a mouthwash containing chlorhexidine to have this antimicrobial agent penetrate down to the tooth surface underneath the center of the plaque? The diffusion coefficient of chlorhexidine in water, as estimated by the Wilke-Chang correlation, is $3.7 \times 10^{-6} \text{ cm}^2 \text{ s}^{-1}$ (34). Holding the mouthwash in the mouth will raise its temperature; assume that the mean temperature is 30°C. The aqueous diffusion coefficient at 30°C is then $4.2 \times 10^{-6} \text{ cm}^2 \text{ s}^{-1}$. From Stewart (33) the value of D_e/D_{aq} in dental plaque for a solute such as chlorhexidine is predicted to be ca. 0.2. This gives a value of D_e of $0.84 \times 10^{-6} \text{ cm}^2 \text{ s}^{-1}$. Using the formula for a sphere ($0.37 R^2/D_e$), which also applies to a hemisphere on an impermeable plane, the diffusion time is calculated to be 298 s. Try swishing mouthwash for this period to develop a new appreciation for just how long 5 min is.

Example calculation. A mixed-species biofilm grown for 6 days is 1,000 μm thick and locally uniform in thickness. Sodium chloride is added to the bulk fluid, and the appearance of the chloride ion is detected by using a microelectrode positioned near the substratum at the base of the biofilm. Estimate how

long it takes for the chloride concentration at the substratum to reach 90% of the bulk fluid concentration. The system temperature is 24°C. The diffusion coefficient of chloride ion in water at 24°C is $20 \times 10^{-6} \text{ cm}^2 \text{ s}^{-1}$. Taking D_e/D_{aq} to be 0.70, D_e is $14 \times 10^{-6} \text{ cm}^2 \text{ s}^{-1}$. The required penetration time is 714 s or almost 12 min. This calculation is based on an experiment reported by Stewart et al. (35), and the calculated time scale is in rough agreement with the experimental result (1,000 s).

Example calculation. An experimenter proposes to test the role of a certain gene in biofilm development by overexpressing the gene at a particular stage in the maturation of the biofilm. The gene is placed under the control of a promoter that can be induced by adding IPTG (isopropyl- β -D-thiogalactopyranoside). This inducer will be added when young microcolonies are forming. These microcolonies can be approximated as hemispherical patches of radius 5 μm . It is desired to calculate any delay in gene expression that might result from the time needed for the IPTG to diffuse throughout the nascent colony. The system temperature is 37°C. IPTG is a modified monosaccharide, so we can estimate from Table 1 that its diffusion coefficient in water at 25°C will be ca. $6.5 \times 10^{-6} \text{ cm}^2 \text{ s}^{-1}$. Scaling to 37°C and taking D_e/D_{aq} to be 0.25, D_e is found to be $2.2 \times 10^{-6} \text{ cm}^2 \text{ s}^{-1}$. The required penetration time is a mere 0.12 s. The delay anticipated for diffusive ingress is negligible.

Having made these calculations, it is now appropriate to disclose the four assumptions implicit in them. Two of the assumptions are particularly critical because they are often invalid. The first of these is that resistance to mass transfer outside of the biofilm can be neglected. In plain language, this means that the concentration of the diffusing solute right at the biofilm surface is essentially the same as its concentration in the well-mixed bulk fluid. The other key assumption is that the solute whose penetration is being analyzed does not sorb or react in the biofilm. Both assumptions, if violated, will cause the actual penetration time to be longer than the calculated time. The preceding calculations, therefore, are best regarded as lower bounds on the actual diffusion time.

These two issues are discussed at greater length in the following paragraphs. The derivation of equations 1 and 2 also assumes an impermeable substratum and a uniform effective diffusivity within the biofilm.

The term external mass transfer resistance refers to the barrier to diffusion posed by slow-moving fluid adjacent to a biofilm. The fluid may be moving, but its direction of flow is generally parallel to the biofilm surface when very close to the biofilm. This means that although there is convective transport in the direction of flow, there is little or no convection in a direction that would carry a solute into or out of a cell cluster. The extent of external mass transfer resistance depends on the hydrodynamics of the system. There is probably little external mass transfer resistance in high-velocity, turbulent flows. External mass transfer resistance is likely important in many laminar flow systems and is assuredly an issue in systems in which the fluid is static. There are quantitative approaches to calculating the effects of external resistance, but these are beyond the scope of this article. Suffice it to say that all of the diffusion-related phenomena discussed in this article will only be exacerbated when external mass transfer resistance is present.

Penetration times calculated by using equation 1 or 2 will be

reasonable estimates as long as there is no significant reaction or sorption of the solute in the biofilm. It may be easiest to appreciate this caveat by considering a couple of examples in which these equations break down. The diffusive penetration of IPTG calculated in the last example above depends on there being no metabolism of this molecule. While sugars have diffusion coefficients in water that are similar to that of IPTG, it would be incorrect to apply the IPTG result to the transport of a sugar if the microorganisms are capable of metabolizing that saccharide. Microbial utilization of the sugar will reduce its concentration as it diffuses into the biofilm. It would also be incorrect, for example, to equate the penetration time for the chloride ion (Cl^-) calculated in the third example above with the penetration time for the hypochlorite ion (OCl^-), even though these two ions have essentially the same diffusion coefficient in water. Whereas the chloride ion is inert, the hypochlorite ion is highly reactive and will be neutralized by reactions with organic matter in the biofilm. These reactions profoundly retard penetration of this species (6, 35). When a solute reacts in the biofilm it may never fully penetrate the biofilm. Reaction and diffusion achieve a steady balance that leads to persistent concentration profiles within the biofilm. This interaction is the subject of the next section.

WHY ARE BIOFILM CHEMISTRY AND BIOLOGY SO SPATIALLY HETEROGENEOUS?

Local variation in the concentrations of metabolic substrates, products, and microbial species is one of the hallmarks of the biofilm mode of growth. Some of the metabolites for which concentration profiles have been experimentally measured in biofilms include oxygen, nitrite, nitrate, ammonium, pH, sulfide, and methane. The slow and spatially heterogeneous growth of microorganisms within biofilms (31, 38, 42) surely results from such nutrient gradients. These same chemical gradients create environmental microniches that allow for the coexistence of diverse species (3). Some examples of the rich ecology that is possible in biofilms are expounded on below.

There are now a few elegant studies in which chemical gradients measured by using microelectrodes have been related to the distribution of specific bacterial species by in situ hybridization to fluorescently labeled oligonucleotide probes (19, 20, 24, 27, 29). These studies confirm that distinct chemical niches exist at different depths in biofilms. They also make it possible to understand how metabolically diverse microorganisms coexist in the biofilm. In nitrifying biofilms, for example, ammonia-oxidizing and nitrite-oxidizing bacteria coexist in close association. Clusters of nitrite oxidizers crowd around distinct clusters of ammonia oxidizers (20, 29). Thus, is the metabolic waste product of the ammonia oxidizers, nitrite, made available to the bacteria that can use it as a substrate for oxidation. The activities of these commingled species lead to the consumption of ammonia and oxygen near the biofilm surface and the simultaneous production and consumption of nitrite slightly below the biofilm surface. Analogous relationships have been developed for biofilms in which sulfate reduction and sulfide oxidation occur (19, 24, 27). The stratified distributions of the bacteria that constitute methanogenic consortia

have also been described and can be understood in terms of the diffusive exchange of metabolites between species (11, 17).

Other phenomena in biofilms that can be understood, at least in part, by analyzing diffusive transport include different patterns of gene expression in comparison to suspended-cell cultures, microbially influenced corrosion, tolerance of antimicrobial agents, and changes in the apparent kinetics of microorganisms growing in biofilms.

It is increasingly clear that bacteria in biofilms display special phenotypes that are reflected at the gene and protein level. Among the genes and proteins that appear to be differentially regulated in biofilms are those involved in metabolism or starvation responses (14, 21, 28, 39, 41). This regulation could easily be the result of incomplete penetration of nutrients or electron acceptors into the biofilm. One mechanism by which patches of bacteria can induce corrosion of ferrous metals is by creating local anaerobic zones on a metal surface that is elsewhere exposed to oxygen. This gives rise to so-called "differential aeration cells" and sets in motion a self-propagating electrochemical cycle that causes dissolution of metal in the anaerobic zones. Two of the leading explanations for the reduced susceptibility of microorganisms in biofilms also depend on reaction-diffusion interactions. Retarded or incomplete penetration of an antimicrobial agent arises when the agent reacts with or sorbs to biomass in the surface layers of the biofilm faster than it diffuses into the biofilm interior. A second mechanism of reduced biofilm susceptibility hinges on gradients in growth rate inside biofilms. Microorganisms in some strata of the biofilm, where nutrients have been locally depleted, may enter a nongrowing state in which they are less susceptible. Changes in the apparent value of a half-saturation coefficient (K_m) or in the apparent reaction order of substrate utilization are common in biofilms and are easily explained by incorporating the process of diffusion.

I now turn to some simple calculations that can describe reaction-diffusion phenomena in a biofilm. The following equations derive from the same assumptions outlined in the previous section, except that the constraint on reaction of the solute has been relaxed and the system is assumed to be at steady state. It is also necessary to assume a form for the intrinsic kinetics of the reaction. In the interest of simplicity, all of the following formulae derive from zero-order kinetics. This means that the reaction rate of the solute does not depend on its concentration. If one thinks in terms of Monod or Michaelis-Menten kinetics, this is the case for substrate concentrations much greater than the half-saturation coefficient (K_m).

When zero-order kinetics prevail, the reacting solute will be depleted at some point in the biofilm, provided the biofilm is thick enough. The penetration depth, a , of a reacting solute in a flat slab is given by

$$a = \left(\frac{2D_e S_p}{k_o} \right)^{1/2} \quad (3)$$

where S_o is the solute concentration at the biofilm-bulk fluid interface and k_o is the volumetric reaction rate of the solute inside the biofilm. When the solute is a substrate for microbial growth the volumetric reaction rate is given by $k_o = \mu X/Y_{xs}$, where μ is the specific growth rate of the microorganism, Y_{xs} is

the yield coefficient of biomass on substrate, and X is the cell density in the biofilm.

For a spherical cell cluster, the position at which a reacting solute is depleted, r_o , is given by the positive, real root of the cubic equation

$$2\left(\frac{r_o}{R}\right)^3 - 3\left(\frac{r_o}{R}\right)^2 + 1 - \frac{6D_e S_o}{k_o R^2} = 0 \quad (4)$$

where R is the cluster radius. The penetration depth is equal to $R - r_o$. A special case is when the cluster is just large enough to cause the solute concentration to go to zero at the center of the cluster. In this case, $r_o = 0$ and the cluster radius, which can be termed the minimum cluster size necessary to deplete the solute in the biofilm, R_{min} , is

$$R_{min} = \left(\frac{6D_e S_o}{k_o} \right)^{1/2} \quad (5)$$

Once again I illustrate the insight offered by these equations with a few example calculations.

Example calculation. Here we will calculate how far oxygen penetrates into a *Pseudomonas aeruginosa* biofilm. The biofilm is treated as a flat slab with a cell density of 12 mg cm^{-3} . The reaction rate of oxygen in this case is given by $k_o = \mu X/Y_{xs}$, where μ is taken as 0.80 h^{-1} (37) and Y_{xO_2} is 0.85 mg of biomass per mg oxygen (1). The volumetric reaction rate of oxygen inside the biofilm (k_o) is thus $3.1 \text{ mg liter}^{-1} \text{ s}^{-1}$. Take the oxygen concentration in the water at the biofilm surface to be close to saturation at 6 mg liter^{-1} . This concentration of oxygen is much larger than the Monod half-saturation coefficient for oxygen uptake, and so the zero-order kinetic model is a valid approximation. The diffusion coefficient of oxygen in water is $2.68 \times 10^{-5} \text{ cm}^2 \text{ s}^{-1}$ at 37°C (10), and the ratio D_e/D_{aq} for oxygen in biofilms averages 0.57 (Fig. 1). This yields a value of the diffusion coefficient in the biofilm of $1.53 \times 10^{-5} \text{ cm}^2 \text{ s}^{-1}$. From equation 3, the penetration depth is $77 \text{ }\mu\text{m}$. This back-of-the-envelope calculation is in reasonable agreement with experimental measurements of dissolved oxygen profiles in such biofilms (8, 37).

Example calculation. It is possible for anaerobic microorganisms to thrive in aerated waters if they take up residence in the depths of a biofilm containing aerobic bacteria that locally deplete oxygen. Consider a pipe in which the dissolved oxygen concentration is 2 mg liter^{-1} . How large must a rounded biofilm cluster of aerobic bacteria be to create a niche where an obligate anaerobe could take root? The bacterial growth rate is 0.5 h^{-1} , the biomass yield on oxygen is 0.125 mg of biomass per mg oxygen, and the biomass density in the biofilm is 20 mg cm^{-3} . Using the same value of D_e as in the previous example, the cluster radius is $25 \text{ }\mu\text{m}$ as determined by equation 5. A biofilm need not be very thick to create anoxic zones and thereby allow the coexistence of aerobes and anaerobes in close association.

Example calculation. How far will hydrogen peroxide penetrate into a biofilm formed by a catalase-positive organism? Suppose that the hydrogen peroxide is delivered at a bulk fluid concentration of 10 mM . As determined by Brown et al. (2), the specific peroxidase activity of uninduced *P. aeruginosa* is ca. 1 mmol per mg of total cell protein per min . The protein density in a *P. aeruginosa* biofilm is ca. 5 mg cm^{-3} . Taking the

diffusion coefficient of hydrogen peroxide in the biofilm as one-half its value in water at 25°C (34), we have $D_e = 7 \times 10^{-6} \text{ cm}^2 \text{ s}^{-1}$. The calculated penetration depth in a flat slab is only 13 μm . This calculation reinforces the possibility that reactive antimicrobials may fail to penetrate biofilms.

The preceding calculations involve the penetration of a solute that is consumed by reaction in the biofilm. There are also problems in which it is interesting to understand the distribution of a metabolic product within the biofilm. While substrates diffuse down a concentration gradient into the biofilm, products diffuse out of the biofilm from high concentrations in the biofilm interior to lower concentrations in the bulk fluid. These two profiles are mathematically related. There is one particularly simple result that can be used to illustrate some phenomena of interest. The concentration of a metabolic product in the depths of a biofilm is given by

$$P = \frac{D_{\text{es}} Y_{\text{ps}} S_o}{D_{\text{ep}}} + P_o \quad (6)$$

where P is the product concentration in the biofilm interior and P_o is the product concentration in the fluid bathing the biofilm. D_{es} denotes the effective diffusivity of the substrate in the biofilm, and D_{ep} denotes the effective diffusivity of the product in the biofilm. This calculation assumes that product formation is stoichiometrically related to the utilization of a substrate; this relation is embodied in the yield coefficient Y_{ps} . This equation gives the product concentration that prevails in any location in the biofilm where the limiting substrate has been depleted. This result is independent of the biofilm geometry; it can be applied equally well to a flat slab or a rounded mushroom. Two example calculations follow.

Example calculation. Consider a staphylococcal biofilm that is fermenting glucose with the production of predominantly lactic acid. It is of interest to know the maximum concentration of this metabolic product that could occur in the biofilm interior. This peak concentration will occur at any spot where glucose has been depleted. Imagining a biomedical application, take the bulk concentration of glucose to be representative of that in blood at 800 mg liter^{-1} . The yield coefficient of lactate on glucose is estimated to be $Y_{\text{ps}} = 1.8$ mol of lactate per glucose or 0.90 mg of lactate per mg of glucose (30). From Table 1, the ratio of the diffusion coefficients of glucose and lactate is estimated to be $D_{\text{es}}/D_{\text{ep}} = 0.64$. Assuming that the bulk fluid concentration of lactate is negligible ($P_o = 0$), we find $P = 550 \text{ mg liter}^{-1}$. This concentration could be high enough to inhibit growth in the biofilm interior, making those cells less susceptible to antibiotics. It also could be sufficiently acid to lower the local pH and induce undesirable reactions in adjacent tissue or materials.

Example calculation. Quorum sensing refers to the ability of bacteria to sense their density by exchanging diffusible communication molecules called autoinducers. Quorum sensing appears to be an important process in biofilms (5), which is not surprising given the high cell densities. Here I will outline a calculation of how many biofilm bacteria might be required to trigger autoinduction by a quorum-sensing mechanism. Assume that the bacteria grow in spherical clusters and that bacteria throughout the cluster generate the signal molecule at a fixed rate. This rate will have either of two levels: a low basal

level prior to autoinduction and a higher level after autoinduction. How large must a preautoinduction cluster become for the concentration of quorum sensing signal to just attain its threshold level? This is another way to ask the question, "How many bacteria constitute a quorum?" This calculation can be tackled by combining equations 5 and 6 to give

$$R_{\text{min}} = \left(\frac{6D_{\text{ep}}P}{k_o Y_{\text{ps}}} \right)^{1/2} \quad (7)$$

where P now indicates the threshold concentration of the autoinducer, D_{ep} its diffusion coefficient in the biofilm, and $k_o Y_{\text{ps}}$ indicates the production rate of the signal. This result assumes that there is no product (autoinducer) in the bulk fluid. The production rate of signal can be equivalently expressed as $k_p X$, where k_p is a per-cell production rate and X is the cell density in the cluster. Let P be 10 μM , D_{ep} be $10^{-6} \text{ cm}^2 \text{ s}^{-1}$, k_p be $10^{-16} \text{ } \mu\text{mol per cell per s}$, and X be $4 \times 10^{11} \text{ cells per cm}^3$. These values are mostly hypothetical. The required cluster radius is 39 μm . There would be a just about 100,000 bacteria in a cluster of this dimension.

Now suppose that the bacteria in this cell cluster respond through quorum sensing and increase the rate of production of the autoinducer. A biofilm cell cluster in which the cells are in an induced state can become smaller than the threshold radius calculated above without losing the autoinduction phenotype. For example, if the production rate of the signal is increased by a factor of 100 times after autoinduction, the cell cluster could become only one-tenth as large without having the autoinducer drop below the threshold concentration. In the example under study, the cell cluster would shrink from 39 μm to only 4 μm in diameter before autoinduction would switch off. We can appreciate by this calculation that quorum sensing in biofilms should exhibit hysteresis (9).

DO WATER CHANNELS IN BIOFILMS ELIMINATE DIFFUSION LIMITATION?

Much has been made over the last decade of the heterogeneous architecture of some biofilms (3, 36). These biofilms are described as clusters of microbial cells that are interspersed with water channels through which liquid flows. It is natural to wonder whether such conduits might ameliorate or even eliminate limitation of diffusive solute transport. Flowthrough water channels can improve solute transport in the immediate lining of the channel, but it does not assure access to the interior of cell clusters. Perhaps the best demonstration of this fact is the direct experimental measurement of oxygen penetration to the base of a biofilm in a void area but failure of the oxygen to penetrate in an adjacent cell cluster (8). Water may course through channels, but it does not percolate the cell clusters themselves. The dense aggregation of bacterial cells and their extracellular polymers within cell clusters precludes fluid flow. This means that water channels can expose the surfaces of clusters or channels but they do not allow free access of solutes to the interior of cell clusters.

Structural heterogeneity in a biofilm changes the geometry of the diffusion problem, but it does not alter the fundamental phenomena. The illustrative calculations presented in this article have all been framed in terms of simple shapes, but the

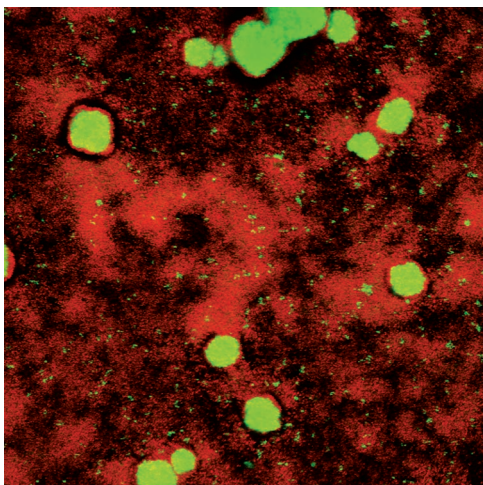


FIG. 2. Spatial pattern of viability in an antimicrobial-treated biofilm. A *Streptococcus mutans* biofilm was treated with a mouthwash and then stained with the BacLight viability indicator. Green cells are "live," and red cells are "dead." The field of view is ca. 500 μm^2 .

ability to calculate diffusion phenomena is not limited by biofilm geometry in this era of fast computers. Several mathematical models have been described that calculate reaction-diffusion interactions in heterogeneous biofilm structures in two dimensions (12, 15, 23).

ARE THERE CRITICAL BIOFILM PHENOMENA THAT DIFFUSION DOES NOT EXPLAIN?

I began this article with the statement that much of what makes life in a biofilm special can be explained by accounting for diffusive phenomena. Diffusion limitation probably does not explain everything though. It is likely that microorganisms have sensing pathways, which trigger gene expression during biofilm development, and that are independent of diffusion-based concentration gradients.

As an approach to this issue, consider the image of an antimicrobial-treated biofilm in Fig. 2. This specimen shows surviving bacteria (green) in the core of mushroom-shaped clusters that sit above a thin base film of killed (red) cells. Why are the survivors concentrated in the interior of cell clusters? One possibility is that the antimicrobial agent failed to penetrate. From what we know about the treatment duration (240 s) and the calculated penetration time (~ 1 s), this explanation is unlikely. Another possibility is that bacteria in the cluster interior are nutrient starved and are less susceptible by virtue of their growth state. This could be simply a matter of slow growth or it could be that "persister" cells are spawned at greater frequency in nutrient-limited environments. A third explanation is that a quorum-sensing signal accumulates in the cluster interior and triggers expression of protective genes. It is worth mentioning that it has recently been postulated that the primary function of quorum sensing is to detect diffusion limitation (25). Certainly, all three of these hypotheses derive fundamentally from diffusion limitation. In the first case, the limitation applies to the antimicrobial agent itself, in the second case it applies to a metabolic substrate, and in the third case it applies to a metabolic product.

Can other pathways to a protected phenotypic state, which do not stem from diffusion limitation, be imagined? Perhaps microorganisms have "touch" sensors on the cell surface that mechanically detect the presence of a solid surface. Another possibility is a feedback mechanism that responds to the increased resistance to motility that must occur when a cell adheres to a surface or is neighbored by other cells and extracellular polymeric substances. Might bacteria have receptors for detecting cell-cell contact? Any of these mechanical sensing mechanisms could potentially initiate a pathway of differentiation, including the generation of cells in protected states. One of the challenges to studying such putative pathways will be demonstration that they indeed operate independent of diffusion phenomena.

SUMMARY

Diffusion in biofilms can be summarized by the following four points.

- (i) Diffusion is the predominant solute transport process within cell clusters.
- (ii) The time scale for diffusive equilibration of a *nonreacting* solute will range from a fraction of a second to tens of minutes in most biofilm systems.
- (iii) Diffusion limitation readily leads to gradients in the concentration of *reacting* solutes and hence to gradients in physiology.
- (iv) Water channels can carry solutes into or out of the depths of a biofilm, but they do not guarantee access to the interior of cell clusters.

ACKNOWLEDGMENTS

This work was supported by a grant from the W. M. Keck Foundation.

The image in Fig. 2 was provided courtesy of Mark Pasmore and Jill Petik.

REFERENCES

1. Bailey, J., and D. Ollis. 1986. Biochemical engineering fundamentals. McGraw-Hill Book Co., New York, N.Y.
2. Brown, S. M., M. L. Howell, M. L. Vasil, A. J. Anderson, and D. J. Hassett. 1995. Cloning and characterization of the *katB* gene of *Pseudomonas aeruginosa* encoding a hydrogen peroxide-inducible catalase: purification of KatB, cellular localization, and demonstration that it is essential for optimal resistance to hydrogen peroxide. *J. Bacteriol.* **177**:6536–6544.
3. Costerton, J. W., Z. Lewandowski, D. de Beer, D. Caldwell, D. Korber, and G. James. 1994. Biofilms, the customized microniche. *J. Bacteriol.* **176**:2137–2142.
4. Cussler, E. L. 1984. Diffusion - mass transfer in fluid systems. Cambridge University Press, Cambridge, United Kingdom.
5. Davies, D. G., M. R. Parsek, J. P. Pearson, B. H. Iglewski, J. W. Costerton, and E. P. Greenberg. 1998. The involvement of cell-to-cell signals in the development of a bacterial biofilm. *Science* **280**:295–298.
6. de Beer, D., R. Srinivasan, and P. S. Stewart. 1994. Direct measurement of chlorine penetration into biofilms during disinfection. *Appl. Environ. Microbiol.* **60**:4339–4344.
7. de Beer, D., P. Stoodley, and Z. Lewandowski. 1997. Measurements of local diffusion coefficients in biofilms by microinjection and confocal microscopy. *Biotechnol. Bioeng.* **53**:151–158.
8. de Beer, D., P. Stoodley, F. Roe, and Z. Lewandowski. 1994. Effects of biofilm structure on oxygen distribution and mass transport. *Biotechnol. Bioeng.* **43**:1131–1138.
9. Dockery, J. D., and J. P. Keener. 2001. A mathematical model for quorum sensing in *Pseudomonas aeruginosa*. *Bull. Math. Biol.* **63**:95–116.
10. Han, P., and D. M. Bartels. 1996. Temperature dependence of oxygen diffusion in H_2O and D_2O . *J. Phys. Chem.* **100**:5597–5602.
11. Harmsen, H. J. M., H. M. P. Kengen, A. D. L. Akkermans, A. J. M. Stams, and W. M. de Vos. 1996. Detection and localization of syntrophic propionate-oxidizing bacteria in granular sludge by in situ hybridization using 16S

- rRNA-based oligonucleotide probes. *Appl. Environ. Microbiol.* **62**:1656–1663.
12. **Hermanowicz, S. W.** 2001. A simple 2D biofilm model yields a variety of morphological features. *Math. Biosci.* **169**:1–14.
 13. **Horvath, A. L.** 1985. Handbook of aqueous electrolyte solutions: physical properties, estimation and correlation methods. John Wiley & Sons, Inc., New York, N.Y.
 14. **Jackson, D. W., K. Suzuki, L. Oakford, J. W. Simecka, M. E. Hart, and T. Romeo.** 2002. Biofilm formation and dispersal under the influence of the global regulator CsrA of *Escherichia coli*. *J. Bacteriol.* **184**:290–301.
 15. **Kreft, J.-U., C. Picioreanu, J. W. T. Wimpenny, and M. C. M. van Loosdrecht.** 2001. Individual-based modeling of biofilms. *Microbiology* **147**:2897–2912.
 16. **Longworth, L. G.** 1955. Diffusion in liquids and the Stokes-Einstein relation, p. 225–247. In T. Shedlovsky (ed.), *Electrochemistry in biology and medicine*. John Wiley & Sons, Inc., New York, N.Y.
 17. **MacLeod, F. A., S. R. Guiot, and J. W. Costerton.** 1990. Layered structure of bacterial aggregates produced in an upflow anaerobic sludge bed and filter reactor. *Appl. Environ. Microbiol.* **56**:1598–1607.
 18. **Mason, C. M., and J. B. Culvern.** 1949. Electrical conductivity of orthophosphoric acid and of sodium and potassium dihydrogen phosphates at 25°C. *J. Am. Chem. Soc.* **71**:2387–2393.
 19. **Okabe, S., T. Itoh, H. Satoh, and Y. Watanabe.** 1999. Analyses of spatial distributions of sulfate-reducing bacteria and their activity in aerobic wastewater biofilms. *Appl. Environ. Microbiol.* **65**:5107–5116.
 20. **Okabe, S., H. Satoh, and Y. Watanabe.** 1999. In situ analysis of nitrifying biofilms as determined by in situ hybridization and the use of microelectrodes. *Appl. Environ. Microbiol.* **65**:3182–3191.
 21. **O'Toole, G. A., K. A. Givvs, P. W. Hager, P. V. Phibbs, Jr., and R. Kolter.** 2000. The global carbon metabolism regulator Crc is a component of a signal transduction pathway required for biofilm development by *Pseudomonas aeruginosa*. *J. Bacteriol.* **182**:425–431.
 22. **Perry, R. H., and C. H. Chilton.** 1973. Chemical engineers' handbook, 5th ed. McGraw-Hill Book Co., New York, N.Y.
 23. **Picioreanu, C., M. C. M. van Loosdrecht, and J. J. Heijnen.** 1998. Mathematical modeling of biofilm structure with a hybrid differential-discrete cellular automaton approach. *Biotechnol. Bioeng.* **58**:101–116.
 24. **Ramsing, N. B., M. Kuhl, and B. B. Jorgensen.** 1993. Distribution of sulfate-reducing bacteria, O₂, and H₂S in photosynthetic biofilms determined by oligonucleotide probes and microelectrodes. *Appl. Environ. Microbiol.* **59**:3840–3849.
 25. **Redfield, R. J.** 2002. Is quorum sensing a side effect of diffusion sensing? *Trends Microbiol.* **10**:365–370.
 26. **Robinson, R. A., and R. H. Stokes.** 1959. Electrolyte solutions. Academic Press, Ltd., London, England.
 27. **Santegoeds, C. M., T. G. Ferdelman, G. Muyzer, and D. de Beer.** 1998. Structural and functional dynamics of sulfate-reducing populations in bacterial biofilms. *Appl. Environ. Microbiol.* **64**:3731–3739.
 28. **Sauer, K., A. K. Camper, G. D. Ehrlich, J. W. Costerton, and D. G. Davies.** 2002. *Pseudomonas aeruginosa* displays multiple phenotypes during development as a biofilm. *J. Bacteriol.* **184**:1154.
 29. **Schramm, A., L. H. Larsen, N. P. Revsbech, N. B. Ramsing, R. Amann, and K.-H. Schleifer.** 1996. Structure and function of a nitrifying biofilm as determined by in situ hybridization and the use of microelectrodes. *Appl. Environ. Microbiol.* **62**:4641–4647.
 30. **Sivakanesan, R., and E. A. Dawes.** 2000. Anaerobic glucose and serine metabolism in *Staphylococcus epidermidis*. *J. Gen. Microbiol.* **118**:143–157.
 31. **Sternberg, C., B. B. Christensen, T. Johansen, A. T. Nielsen, J. B. Andersen, M. Givskov, and S. Molin.** 1999. Distribution of bacterial growth activity in flow-chamber biofilms. *Appl. Environ. Microbiol.* **65**:4108–4117.
 32. **Stewart, P. S.** 1996. Theoretical aspects of antibiotic diffusion into microbial biofilms. *Antimicrob. Agents Chemother.* **40**:2517–2522.
 33. **Stewart, P. S.** 1998. A review of experimental measurements of effective diffusive permeabilities and effective diffusion coefficients in biofilms. *Biotechnol. Bioeng.* **59**:261–272.
 34. **Stewart, P. S., G. A. McFeters, and C.-T. Huang.** 2000. Biofilm control by antimicrobial agents, p. 373–405. In J. D. Bryers (ed.), *Biofilms*, 2nd ed. John Wiley & Sons, Inc., New York, N.Y.
 35. **Stewart, P. S., Rayner, J., Roe, F., and W. M. Rees.** 2001. Biofilm penetration and disinfection efficacy of alkaline hypochlorite and chlorosulfamates. *J. Appl. Microbiol.* **91**:525–532.
 36. **Stoodley, P., D. de Beer, and Z. Lewandowski.** 1994. Liquid flow in biofilm systems. *Appl. Environ. Microbiol.* **60**:2711–2716.
 37. **Walters, M. C., F. Roe, A. Bugnicourt, M. J. Franklin, and P. S. Stewart.** Contributions of antibiotic penetration, oxygen limitation, and low metabolic activity to the tolerance of *Pseudomonas aeruginosa* biofilms to ciprofloxacin and tobramycin. *Antimicrob. Agents Chemother.*, in press.
 38. **Wentland, E. J., P. S. Stewart, C.-T. Huang, and G. A. McFeters.** 1996. Spatial variations in growth rate within *Klebsiella pneumoniae* colonies and biofilm. *Biotechnol. Prog.* **12**:316–321.
 39. **Whiteley, M., M. G. Banger, R. E. Bumgarner, M. R. Parsek, G. M. Teitzel, S. Lory, and E. P. Greenberg.** 2001. Gene expression in *Pseudomonas aeruginosa* biofilms. *Nature* **413**:860–864.
 40. **Wood, B. D., M. Quintard, and S. Whitaker.** 2002. Calculation of effective diffusivities for biofilms and tissues. *Biotechnol. Bioeng.* **77**:495–516.
 41. **Xu, K. D., M. J. Franklin, C.-H. Park, G. A. McFeters, and P. S. Stewart.** 2001. Gene expression and protein levels of the stationary phase sigma factor, RpoS, in continuously fed *Pseudomonas aeruginosa* biofilms. *FEMS Microbiol. Lett.* **199**:67–71.
 42. **Xu, K. D., P. S. Stewart, F. Xia, C.-T. Huang, and G. A. McFeters.** 1998. Spatial physiological heterogeneity in *Pseudomonas aeruginosa* biofilm is determined by oxygen availability. *Appl. Environ. Microbiol.* **64**:4035–4039.

The views expressed in this Commentary do not necessarily reflect the views of the journal or of ASM.